Indicators evaluating thermal inertia performance of envelops with phase change material

Haoshu Ling[a,*], Chao Chen[a,*], Hong Qin [b], Shen Wei[c], Jie Lin [a], Na Li[a], Mingxing Zhang[a], Nan Yu [a], Yin Li[a]

[a] *College of Architecture and Civil Engineering, Beijing University of Technology, Beijing 100124, P R China*

[b] *Department of Construction Engineering, Guangzhou Vocational College of Science and Technology, Guangzhou 510450, PR China*

c Faculty of Engineering and Environment, Northumbria University, Newcastle Upon Tyne, NE1 8ST, United Kingdom

Abstract

Phase change material (PCM) has been widely integrated in building envelops to increase their thermal inertia performance. To evaluate the thermal inertia performance of materials and envelops, Chinese Thermal Design Code has provided three indicators, namely, thermal storage coefficient, thermal resistance and thermal inertia index. The existing simplified method calculating the thermal storage coefficient is only applicable for materials with constant thermal properties. For those with varying thermal

* Corresponding author. Tel.: +86 10 67391608-201; fax: +86 10 67391608-201.
E-mail address: linghaoshu@163.com(H. Ling); chenchao@bjut.edu.cn(C. Chen)

properties, such as PCM, however, further developments are still required. To solve this issue, both dimensional analysis and numerical simulation were carried out to develop relationships between the thermal storage coefficient of PCM and its other thermal properties (e.g. thermal conductivity, density and the effective equivalent specific heat). Based on the developed relationships, a simplified method calculating the thermal storage coefficient of PCM was proposed in this study. This simplified method was then combined into the thermal inertia index for evaluating the thermal inertia performance of building envelops with PCM.

Keywords: Phase change material; Thermal inertia performance; Thermal storage coefficient; Dimensional analysis; Building simulation

Nomenclature

C	constant
c	specific heat capacity (J/kg °C)
D	thermal inertia index
k	thermal conductivity (W/m °C)
kg	dimension of mass
m	dimension of length
q	heat flux (W/m^2)
R	thermal resistance (m^2 °C/W)

44	s	dimension of time
45	t	temperature (°C)
46	TSC	thermal storage coefficient (W/m^2 °C)
47	x	independent variable
48	y	variable
49	Z	periodic time of the heating effect (s)
50	ρ	density (kg/m^3)
51	δ	thickness (m)
52	τ	time (s)
53	$°C$	dimension of temperature
54	Δh	enthalpy difference (kJ/kg)
55	Δt	temperature difference (°C)

56

57 **Subscripts**

58	*Br*	brick
59	*i*	node position or serial number
60	*In*	polystyrene board
61	*max*	maximum
62	*min*	minimum
63	*n*	serial number
64	*PCM*	phase change material
65	*sum*	sum

66	*wall*	wall
67	*wall, in*	inner surface of wall
68	*wall, out*	outer surface of wall
69		
70	**Superscript**	
71	*j*	time coordinate
72		
73	*Abbreviations*	
74	PCM	**P**hase **C**hange **M**aterial
75	EVAC	**E**thylene **V**inyl-**A**cetate **C**opolymer

1. Introduction

Phase change material (PCM) has been widely integrated in building envelopes [1-5], thanks to its ability of increasing the thermal inertia performance of building components [6-9], hence improving indoor thermal comfort [10-14]. In the past several decades, many studies have been carried out to explore the effectiveness of PCM on improving indoor thermal comfort in buildings [15-18]. Ling et al [15] explored this in solar greenhouses with and without PCM, using both experimental and numerical methods. From the study, they confirmed a significant contribution of PCM to enhancing the indoor thermal environment under different weather conditions and over a long time, with a maximum increasing rate of 15.3% for the daily effective accumulative temperature. Shi et al [16] presented results from an experimental investigation on macro-encapsulated PCM that has been incorporated in concrete walls in real rooms, and they found out that the maximum temperature and the relative humidity were decreased by up to 4°C and 16%, respectively, in the room with PCM, comparing to that without PCM. Castell and Farid [17] assessed the effectiveness of using PCM in passive cooling building envelopes. From the study, they reported that the building with PCM had a lower risk of thermal discomfort, and this result was supported by Evola et al [18].

Existing studies on the thermal inertia performance of building envelops focused on evaluating their ability with respect to both heat storage and thermal insulation. Ling et

al [15] developed an one-dimensional unsteady numerical heat transfer model for calculating the daily heat storage of external walls with PCM in solar greenhouses. They reported that PCM provided a great contribution to the overall thermal storage of the wall (the daily heat storage rate of PCM during daytime on sunny and cloudy days were 78.1% and 80.3%, respectively). Zhou et al [19] carried out a thermal evaluation of a non-deform laminated composite gypsum board that consists of a 4mm PCM layer in a naturally ventilated condition, and they figured out that the maximum energy storage reached to 363.7 kJ/m^2. In mid-western Greece, Mandilaras et al [20] have built a two-storey typical family house with PCM in the external walls. Their experimental data reflected that the thermal insulation performance of the walling system was promoted in late spring, early summer and autumn, due to the use of PCM. Additionally, the decrement factor decreased by a further 30-40% and the time lag increased for about 100 minutes. Zhou et al [21, 22] have investigated both temperature wave and heat flux wave on the inner surface of shape-stabilized PCM wallboards with sinusoidal temperature wave and heat flux wave on the outer surface, and compared the results with those from conventional building materials such as brick and foam concrete. From both investigations, they found out that PCM wallboards provided the longest time lag and the lowest decrement factor.

To evaluate the thermal inertia performance of materials and envelops, Chinese Thermal Design Code for Civil Buildings (GB 50176-201X) [23] has provided three indicators, namely, thermal storage coefficient, thermal resistance and thermal inertia

120 index. Wang et al [24], Kong et al [25] and Feng [26] have adopted these indicators
121 when evaluating the thermal inertia performance of building envelops made of
122 materials with constant thermal properties. To estimate the thermal storage coefficient,
123 a simplified calculation method has been given in the standard. For materials with
124 constant thermal properties, e.g. soil and cement mortar, this method can be attained
125 using Laplace transform [27]. However, for PCM that has changing equivalent specific
126 heat capacity during the phase change process [28, 29], its thermal storage coefficient
127 can't be estimated using the current method provided.
128
129 This study is aiming to further develop the existing simplified calculation method in
130 the Chinese standard for estimating the thermal storage coefficient for materials with
131 changing thermal properties, focusing on PCM. In the study, relationships between the
132 thermal storage coefficient of PCM and its other thermal properties (e.g. thermal
133 conductivity, density and effective equivalent specific heat) were developed using the
134 Rayleigh's method of dimensional analysis. Additionally, the thermal storage
135 coefficient of PCM with different thermal properties was predicted by EnergyPlus [30],
136 a popular dynamic building performance simulation tool. Combining results of both
137 dimensional analysis and numerical simulation, an updated simplified method
138 calculating the thermal storage coefficient of PCM was proposed. Finally, a case study
139 using this updated method to evaluate the thermal inertia performance of existing
140 materials and envelops was introduced.
141

2. Evaluating the thermal inertia performance of building envelopes

Building envelops link outdoor environment and indoor environment. Generally, the outer surface of building envelopes gains/losses heat from/to the outdoor thermal environment through two main mechanisms, namely, heat radiation and heat convection. The direction of heat transfer (whether gain or loss heat) depends on the temperature of the outer surface of envelops, the outdoor dry-bulb temperature, the surface temperature of surroundings and solar radiation. When the outer surface of envelops gains/losses heat, its temperature will increase/decrease. The heat transfer between indoors and outdoors is mainly driven by heat conduction, depending on the surface temperatures of inner and outer surfaces. When the temperature of outer surface is higher than the inner surface's, heat is transferred into the building so the indoor environment gains heat from outdoors, and vice versa. According to these basic heat transfer theories, in order to evaluate the thermal inertia performance of building envelops, an indicator is needed which can evaluate the materials' ability of both resisting heat transfer between indoors and outdoors and storing excessive heat either gained from outdoors or generated from indoors.

2.1. Thermal inertia index

Thermal inertia index is an indicator that is used to evaluate the ability of both resisting heat transfer through the building envelops and storing excessive heat either gained

from outdoors or generated from indoors. It is defined as the product of the thermal resistance and the heat storage coefficient of materials. The thermal inertia index of laminated composite envelops with PCM is determined as the numerical sum of thermal inertia index of each material layer, as defined in Eq.1.

$$D_{sum} = \sum D_i = \sum TSC_i \cdot R_i \quad (1)$$

2.2. Thermal resistance

Thermal resistance is a parameter evaluating the ability of envelops resisting heat transfer. It is dependent on the material's thickness and thermal conductivity. The thermal conductivity of PCM changes insignificantly during the phase change process due to microencapsulation [31], so it can be considered as a constant. The same as thermal inertia index, the thermal resistance of laminated composite envelops with PCM is a numerical sum of thermal resistance of each material layer, which is calculated using Eq.2.

$$R_{sum} = \sum R_i = \sum \frac{\delta_i}{k_i} \quad (2)$$

2.3. Thermal storage coefficient

The thermal storage coefficient evaluates the materials' ability of storing excessive heat

either gained from outdoors or generated from indoors, defined as the ratio of surface heat flux amplitude to surface temperature amplitude, when materials with infinite thickness are heated with periodic fluctuation (Eq.3).

$$TSC = \frac{q_{\max} - q_{\min}}{t_{\max} - t_{\min}} \tag{3}$$

For materials with constant thermal properties, Eq.3 can be simplified to be Eq.4 using Laplace transform [27], which reflects that the thermal storage coefficient of a material is mainly dependent on its thermal conductivity, density and specific heat capacity.

$$TSC = \sqrt{\frac{2\pi k \rho c}{Z}} \tag{4}$$

For materials with inconstant thermal properties, such as PCM that has changing equivalent specific heat capacity during the phase change process [27, 28], Eq.3 cannot be simplified using the Laplace transform method, so Eq.4 is not suitable for calculating the thermal storage coefficient of PCM. Therefore, the simplified calculation method needs to be further developed so it can be used for estimating the thermal storage coefficient of PCM.

3. Simplified calculation method of thermal storage coefficient of PCM

To expand the above simplified calculation method for PCM, correlations between the thermal storage coefficient of PCM and its other thermal properties (e.g. thermal conductivity, density and effective equivalent specific heat) were determined, using the Rayleigh's method that is one of the dimensional analysis methods. Taking an external wall with PCM in the solar greenhouse as an example, the surface heat flux/temperature amplitudes were generated by EnergyPlus software [30], and the thermal storage coefficient of PCM with different thermal properties were calculated by Eq.3. Then combining results from both dimensional analysis and numerical simulation, a simplified calculation method of thermal storage coefficient of PCM can be proposed.

3.1. Relationships between thermal storage coefficient of PCM and its other thermal properties by dimensional analysis

3.1.1. Dimensional analysis

The dimensional analysis is carried out by analyzing the correlations between different physical quantities by identifying their fundamental dimensions and units of measure and tracking these dimensions as calculations or comparisons [32]. The Rayleigh's method is a key theorem in dimensional analysis, which is named after Lord Rayleigh [33].

If y is a variable that depends upon independent variables x_1, x_2, x_3, ..., x_n, in the form

229 defined below,

230

231 $$y = f(x_1, x_2, x_3, ..., x_n) \quad (5)$$

232

233 Then the fundamental dimension of the above equation is written as Eq.6, and the
234 functional equation is written as Eq.7.

235

236 $$\dim y = (\dim x_1)^{c_1} (\dim x_2)^{c_2} (\dim x_3)^{c_3} ... (\dim x_n)^{c_n} \quad (6)$$

237

238 $$y = C x_1^{c_1} x_2^{c_2} x_3^{c_3} ... x_n^{c_n} \quad (7)$$

239

240 3.1.2. Calculating thermal storage coefficient of PCM by dimensional analysis

241

242 According to the simplified calculation method of materials with constant thermal
243 properties (Eq.4), the thermal storage coefficient is influenced by periodic time of
244 heating effect, specific heat, thermal conductivity and density. In practice, the heating
245 effect influencing building envelops mainly includes solar radiation and outdoor air
246 temperature, whose periodic time is 24h (86400s). Similar to materials with constant
247 thermal properties, PCM also has the constant thermal conductivity and density during
248 the phase change process. However, each PCM has a specific phase change temperature
249 and changing equivalent specific heat under different temperature conditions. When the
250 temperature of PCM reaches the phase change temperature, the heat is stored in the

form of latent heat. Therefore, the physical quantity characterizing the heat capacity per unit mass of PCM should be the effective equivalent specific heat, which is equal to the ratio of the enthalpy difference to the resulting temperature difference. Fig.1 shows the correlation between the equivalent specific heat and the temperature of one specific type of PCM, which was used in this study. It is a kind of shape-stabilized solid-liquid PCM made of paraffin wax, expanded graphite, high density polyethylene and cement mortar. It has a phase change temperature ranging between 7.1°C and 25.9°C, with a heat of fusion of 128.1kJ/kg. When the t_{min} and t_{max} can be determined in real application, which are dependent on the amount of fluctuated heat supplied, the enthalpy difference is the area enclosed by the correlation and the x-axis, Δh shown in Fig.1, so the effective equivalent specific heat can be calculated by Eq.8.

$$\frac{\Delta h}{\Delta t} = \frac{\int_{t_{\min}}^{t_{\max}} c(t)dt}{t_{\max} - t_{\min}} \tag{8}$$

Therefore, it could be assumed that the thermal storage coefficient of PCM is influenced by periodic time of heating effect, thermal conductivity, density, and effective equivalent specific heat of PCM, so in the form of,

$$TSC = f(Z, k, \rho, \frac{\Delta h}{\Delta t}) \tag{9}$$

According to Eq.9, dimensions of all quantities can be expressed as the product of the basic physical dimensions length, mass, time and temperature, represented by symbols

273 *m*, *kg*, *s* and °*C*, respectively. Therefore, fundamental dimensions of these quantities are,

274

275 $$\dim TSC = kg \cdot s^{-3} \cdot {}^{\circ}C^{-1} \tag{10}$$

276

277 $$\dim Z = s \tag{11}$$

278

279 $$\dim k = kg \cdot m \cdot s^{-3} \cdot {}^{\circ}C^{-1} \tag{12}$$

280

281 $$\dim \rho = kg \cdot m^{-3} \tag{13}$$

282

283 $$\dim \frac{\Delta h}{\Delta t} = m^2 \cdot s^{-2} \cdot {}^{\circ}C^{-1} \tag{14}$$

284

285 Then the fundamental dimension of Eq.9 could be written as,

286

287 $$kg \cdot s^{-3} \cdot {}^{\circ}C^{-1} = s^{c_1} \cdot (kg \cdot m \cdot s^{-3} \cdot {}^{\circ}C^{-1})^{c_2} \cdot (kg \cdot m^{-3})^{c_3} \cdot (m^2 \cdot s^{-2} \cdot {}^{\circ}C^{-1})^{c_4} \tag{15}$$

288

289 According to the dimensional homogeneity, a set of simultaneous equations are

290 obtained:

291

292 $$\begin{cases} kg: & 1 = C_2 + C_3 \\ s: & -3 = C_1 - 3C_2 - 2C_4 \\ {}^{\circ}C: & -1 = -C_2 - C_4 \\ m: & 0 = C_2 - 3C_3 + 2C_4 \end{cases} \tag{16}$$

293

The solutions of the simultaneous equations above are,

$$\begin{cases} C_1 = -\dfrac{1}{2} \\ C_2 = C_3 = C_4 = \dfrac{1}{2} \end{cases} \tag{17}$$

Then the simplified calculation method of the thermal storage coefficient of PCM could be written as Eq.18.

$$TSC = C\sqrt{\frac{1}{Z}}\sqrt{\rho}\sqrt{k}\sqrt{\frac{\Delta h}{\Delta t}} \tag{18}$$

Where *C* is a constant.

When the constant *C* is determined, the thermal storage coefficient of PCM can be also determined, and this is the expanded simplified calculation method developed in this study.

3.2. Determining constant C using building simulation

To determine the constant *C* in Eq. 18, the surface heat flux/temperature amplitudes of PCM integrated in external walls of a solar greenhouse were derived from EnergyPlus software [30], and then the thermal storage coefficient of PCM with different thermal properties were calculated using Eq.3.

315

316 3.2.1. Simulation model

317

318 The simulation model used in this study was built upon a solar greenhouse located in
319 Beijing (40 °N, 116 °E), China, with a length of 28.6m and a width of 6.7m, as shown
320 in Fig.2. It consisted of a solid north wall, a partial roof on the top of the north wall and
321 a cover over the south part of the solar greenhouse. Its north wall has a height of 2.3m
322 and was formed of three layers: polystyrene boards, block bricks and PCM, from
323 outside to inside respectively. The cover was made of three transparent ethylene vinyl-
324 acetate copolymer films with a thickness of 0.1mm, allowing solar energy go into the
325 greenhouse during the daytime (09:00 to 16:00). During the night time (16:00 to 09:00
326 day+1), a 40.0mm thick cotton blanket would be added onto the top of the cover to
327 reduce heat loss [34]. Therefore, the temperature of the inner surface of the north wall
328 was affected by the indoor thermal environment of the solar greenhouse and solar
329 radiation. On the top of the south roof, there was a bar vent that was opened between
330 11:00 and 14:00 to release excessive heat and humidity. Physical parameters of
331 materials used in the greenhouse are provided in Table 1.

332

333 The thermal performance of the PCM used in this study that has a thickness of 50mm
334 has already been studied and presented by Ling et al [15] and Guan [35], based on the
335 measurement of outdoor air temperature, solar radiation, and the surface temperature
336 of PCM. In order to verify the prediction accuracy of the simulation package, the real-

337 measured outdoor air temperature and the solar radiation from the previous study have
338 been used to drive the simulation, replacing the default weather data in EnergyPlus.
339 Fig.3 shows the winter weather data used for the later simulation work, with three sunny
340 days and two cloudy days. During this period, the outdoor air temperature varied
341 between -6.4 °C and 4.5 °C for sunny days and between -7.4 °C and -0.2 °C for cloudy
342 days; the maximum solar radiation was 566 W/m^2 for sunny days and 326 W/m^2 for
343 cloudy days.
344
345 3.2.2. Simulation definitions
346
347 To verify the accuracy of the simulation results, the following simulation conditions
348 were used for the model calibration, as listed in Table 2. Case 1 was the same as the
349 experimental conditions introduced in the previous study [15, 35]. In this case, the
350 predicted surface temperature of PCM by EnergyPlus was compared with that collected
351 from the field experiment. However, Case 1 did not meet the requirement of infinite
352 thickness of PCM when evaluating their thermal storage coefficient [35]. Therefore, in
353 Case 2, the thickness of PCM was extended greatly. Other cases were defined for
354 estimating the thermal storage coefficient of PCM under various other conditions,
355 namely various density (Case 3), thermal conductivity (Case 4) and effective equivalent
356 specific heat (Case 5), under the climatic conditions measured on January 26, due to
357 the high temperature and solar radiation on that day, which can promote the contribution
358 of PCM to the indoor thermal environment.

3.2.3. Model calibration

To calibrate the simulation model built for the case study building, the predicted surface temperature of PCM by EnergyPlus under the simulation conditions defined in Case 1, Table 2 was compared with that field measured from the previous study [15, 35], as shown in Fig.4. The comparison depicts a good agreement between the measured and simulated temperatures, with an average temperature difference of 0.1°C.

3.2.4. Validation of infinite thickness

As the method proposed in this study (Eq.3) is used to evaluate the thermal storage coefficient of PCM, with a requirement of infinite thickness of the material, the prediction results by EnergyPlus with a thickness of 200mm of PCM (Case 2, Table 2) needed to be validated as suitable to represent the thermal conditions at infinite thickness. To demonstrate the suitability, the inner and outer surface temperatures of the external wall with PCM in the solar greenhouse were used as the boundary conditions, and the temperature distribution along the thickness direction of the wall was calculated using a one-dimensional unsteady numerical heat transfer model defined in Eq. 19, according to basic theories of thermal conduction [36].

$$\rho \frac{\partial (ct)}{\partial \tau} = \frac{\partial}{\partial \delta}(k \frac{\partial t}{\partial \delta}) \tag{19}$$

With boundary conditions as,

$$t|_{\delta=0} = t_{wall,in} \tag{20}$$

$$t|_{\delta=\delta_{wa}} = t_{wall,out} \tag{21}$$

To solve the above equations, the explicit finite difference method was adopted, and the equation was discretized as,

$$\frac{\rho_i(c_i^j t_i^j - c_i^{j-1} t_i^{j-1})}{\Delta\tau} = \frac{k_{i+1} t_{i+1}^j - 2k_i t_i^j + k_{i-1} t_{i-1}^j}{\Delta\delta^2} \tag{22}$$

Where $\Delta\tau$ and $\Delta\delta$ were time step (600s) and mesh size (0.005m), respectively.

Since the wall with PCM was heterogeneous, thermal properties of materials at different positions were given as,

$$\begin{cases} c_i = c_{PCM}, \quad \rho_i = \rho_{PCM}, k_i = k_{PCM} & if \quad 0 \le i \le 40 \\ c_i = c_{Br}, \quad \rho_i = \rho_{Br}, k_i = k_{Br} & if \quad 40 < i \le 200 \\ c_i = c_{In}, \quad \rho_i = \rho_{In}, k_i = k_{In} & if \quad 200 < i \le 210 \end{cases} \tag{23}$$

The above unsteady numerical heat transfer model has been validated in our previous study. A good agreement between the measured and calculated temperatures has been

observed [15].

Using EnergyPlus, the inner and outer surface temperatures of the wall with PCM in the solar greenhouse were predicted under the simulation conditions defined in Case 2, Table 2. Then the temperature distribution along the thickness direction was calculated, using the above unsteady numerical model. The calculation result for the 200mm PCM layer is shown in Fig.5, which reflects that with the increase of thickness of PCM, the temperature amplitude was decreasing. The maximum surface temperature amplitude of PCM was 18.6°C, happened when the thickness was small. However, it was less than 0.5°C, when the thickness is 200mm. This means that the heating effect of periodic fluctuation had little influence on PCM when its thickness was beyond 200mm. Therefore, the 200mm thick PCM integrated in the wall was considered to meet the requirement of the infinite thickness.

3.2.5. Simulation results

3.2.5.1. Influence of density

To evaluate the influence of the density of PCM on the thermal storage coefficient, the surface heat flux/temperature amplitudes of PCM with different density were predicted by EnergyPlus under the simulation conditions defined in Case 3, Table 2, and then the thermal storage coefficient was calculated using Eq.3.

The surface heat flux/temperature amplitudes of PCM with different density are presented in Fig. 6, which reflects that the density of PCM was indirectly proportional to the temperature amplitude, and it was directly proportional to the heat flux amplitude. Therefore, with the increase of density, the thermal storage coefficient of PCM increased. Furthermore, using the least square method, the thermal storage coefficient of PCM was found to be proportional to the square root of the density, as shown in solid line through round dots Fig.6, similar to materials with constant thermal properties. The correlation equation is defined in Eq.24. This also met the result of the dimensional analysis introduced in Section 3.1.

$$TSC = 0.5104\sqrt{\rho} \qquad R^2 = 0.9982 \tag{24}$$

Combining results from both simulation and dimensional analysis, when Z=86400s, k=0.54W/(m °C), and $\Delta h/\Delta t$=7.06±0.95kJ/(kg °C), the formula of thermal storage coefficient of PCM was written as,

$$TSC = C\sqrt{\frac{1}{Z}}\sqrt{k}\sqrt{\frac{\Delta h}{\Delta t}}\sqrt{\rho} = 0.5104\sqrt{\rho} \tag{25}$$

So, $C \approx \sqrt{2\pi}$

3.2.5.2. Influence of thermal conductivity

In order to analyze the influence from the thermal conductivity of PCM on the thermal storage coefficient, the surface heat flux/temperatures amplitudes were predicted by EnergyPlus under the simulation conditions defined in Case 4, Table 2. The same as above, the thermal storage coefficient of PCM with different thermal conductivity was calculated using Eq. 3. Fig.7 shows the prediction results, which reflects that when the thermal conductivity of PCM increased, the heat transfer was promoted. Under the same heating periodic fluctuation, the surface temperature of PCM with bigger thermal conductivity became stable, also with a strengthened heat storage/release ability. Therefore, the thermal conductivity showed a positive influence on the surface heat flux amplitude, a negative influence on the surface temperature amplitude and a positive influence on the thermal storage coefficient. The relationship between them was represented by Eq. 26, based on the predicted data.

$$TSC = 20.979\sqrt{k} \qquad R^2 = 0.9976 \tag{26}$$

Combining results from both simulation and dimensional analysis, when Z=86400s, ρ=900 kg/m^3, $\Delta h/\Delta t$=7.21±0.93 kJ/(kg °C), the formula of thermal storage coefficient of PCM was written as,

$$TSC = C\sqrt{\frac{1}{Z}}\sqrt{\rho}\sqrt{\frac{\Delta h}{\Delta t}}\sqrt{k} = 20.979\sqrt{k} \tag{27}$$

So, $C \approx \sqrt{2\pi}$

3.2.5.3. Influence of effective equivalent specific heat

According to the simulation conditions defined in Case 5, Table 2, the surface heat flux/temperatures amplitudes of PCM with different effective equivalent specific heat were predicted, and the thermal storage coefficient of PCM was calculated by Eq. 3. Fig. 8 shows the change of the thermal storage coefficient, the surface heat flux amplitude and the temperature amplitude of PCM with different effective equivalent specific heat. The prediction results reflect that the more effective equivalent specific heat was, the softer the surface temperature amplitude of PCM was, but the stronger the surface heat flux amplitude was. Therefore, the effective equivalent specific heat of PCM had the same effect on the thermal storage coefficient as that of materials with constant thermal properties. The correlation was defined by Eq.28, the same as the result obtained from the dimensional analysis introduced in Section 3.1

$$TSC = 0.1864\sqrt{\frac{\Delta h}{\Delta t}} \qquad R^2 = 0.9956 \tag{28}$$

Combining results from both simulation and dimensional analysis, when Z=86400s, ρ=900 kg/m^3, k=0.54W/(m °C), the formula of thermal storage coefficient of PCM was written as,

$$TSC = C\sqrt{\frac{1}{Z}}\sqrt{\rho}\sqrt{k}\sqrt{\frac{\Delta h}{\Delta t}} = 0.1864\sqrt{\frac{\Delta h}{\Delta t}} \quad (29)$$

So, $C \approx \sqrt{2\pi}$

As all simulation conditions indicated $C \approx \sqrt{2\pi}$, substituting it into Eq. 18 gives Eq.30, the further developed simplified calculation method evaluating the thermal storage coefficient of PCM.

$$TSC = \sqrt{\frac{2\pi}{Z}\rho k\frac{\Delta h}{\Delta t}} \quad (30)$$

According to the above equation (Eq.30), it could be found that the thermal storage coefficient of PCM is general proportional to the square root of thermal properties, namely density, thermal conductivity and effective equivalent specific heat. Therefore, an optimization process of finding the best wall with PCM could be based on a combinational consideration of available ranges of these thermal properties in a real application.

4. A case study using the further developed method

This section demonstrates the use of the further developed simplified calculation method for evaluating the thermal performance of building envelopes with PCM, using

511 a real case study as an example. The evaluation work consists of two steps: 1) evaluating
512 the thermal storage coefficient of materials (Section 4.1) and 2) evaluating the thermal
513 inertia performance of building envelops using the calculated thermal storage
514 coefficient (Section 4.2).
515
516 4.1 Evaluating the thermal storage coefficient of materials
517
518 The surface temperature of PCM with a thickness of 50mm in the above solar
519 greenhouse has been measured and presented in our previous study [15], and it was
520 varying between 10.6°C and 26.4°C on a typical sunny day. According to the equivalent
521 specific heat of PCM shown in Fig.1, the effective equivalent specific heat could be
522 calculated as,
523
524 $$\frac{\Delta h}{\Delta t}=\frac{\int_{t_{\min}}^{t_{\max}} c(t)dt}{t_{\max}-t_{\min}}=\frac{\int_{10.6}^{26.4} c(t)dt}{26.4-10.6}=7.42\text{kJ}/\left(\text{kg }^{\circ}\text{C}\right) \quad (31)$$
525
526 At present, materials used in the case study building mainly include PCM, soil, block
527 bricks, polystyrene boards. Using Eq.4 (existing method for materials with constant
528 thermal properties) and Eq. 30 (developed method for materials with varying thermal
529 properties), the thermal storage coefficient of each material was calculated and listed in
530 Table 3. The calculation results reflect that polystyrene boards are the weakest in storing
531 excessive heat either gained from outdoors or generated from indoors, due to its weak
532 values in thermal conductivity, density, special heat and thermal storage coefficient.

533 This is also a reason why lightweight envelops give significant temperature amplitude
534 when heated with periodic fluctuation. PCM has less thermal conductivity and density
535 than soil and block bricks, but it has much bigger effective equivalent specific heat.
536 Therefore, it has a thermal storage coefficient of 16.20 W/(m^2 °C), 1.24 times bigger
537 than soil and 1.54 times bigger than block bricks. Furthermore, it should also be noticed
538 that the thermal conductivity of PCM is less than that of soil and block bricks, meaning
539 that PCM has a better thermal resistance than soil and block bricks, when they have the
540 same thickness. Therefore, when integrated in building envelops, PCM can not only
541 enhance envelops' ability of storing excessive heat, but also strengthen the thermal
542 insulation of envelops.
543
544 4.2 Evaluating the thermal inertia performance of building envelops
545
546 There are four main types of envelops for solar greenhouses. They are all constructed
547 by block bricks and polystyrene boards, but with different thickness of block bricks. In
548 order to evaluate the effectiveness of PCM on improving the thermal inertia
549 performance of building envelops, block bricks are replaced by PCM with the same
550 thickness. Then their thermal resistance and thermal inertia index are calculated using
551 the thermal properties calculated in Section 4.1 and are listed in Table 4. The results
552 reflect that the thickness of materials has a positive influence on both thermal resistance
553 and thermal inertia index, when envelops are made of the same materials. This means
554 that increasing construction thickness is an efficient way of improving the thermal

555 inertia performance of envelops. Additionally, using PCM in envelops can also get the
556 same effect, as when the block bricks are replaced by PCM with the same thickness,
557 both thermal resistance and thermal inertia index go up. When increasing the thickness
558 of PCM, the growth rates of both thermal resistance and thermal inertia index increases
559 as well.
560
561 **5. Conclusions**
562
563 Thanks to the ability of promoting the thermal inertia performance of building
564 components, PCM has been integrated in building envelopes to reduce the buildings'
565 energy demand and improve their indoor thermal environment. Chinese Thermal
566 Design Code for Civil Buildings (GB 50176-201X) has provided three indicators,
567 namely, thermal storage coefficient, thermal resistance and thermal inertia index, to
568 evaluate the thermal inertia performance of materials and envelops. The evaluation
569 adopts a simplified calculation method to evaluate the thermal storage coefficient of
570 materials. This method is only applicable for materials with constant thermal properties.
571 For those with varying thermal properties, such as PCM, however, further
572 developments are still required. To solve this issue, both dimensional analysis and
573 building simulation were applied, and a further development on the existing simplified
574 calculation method has been carried out, based on relationships between the thermal
575 storage coefficient of PCM and its other thermal properties (e.g. thermal conductivity,
576 density and the effective equivalent specific heat). The further developed calculation

577 method has the form of

578

579 $$TSC = \sqrt{\frac{2\pi}{Z}\rho k\frac{\Delta h}{\Delta t}}$$

580

581 In order to demonstrate how to use this method for solving real problems, a case study
582 has been performed as introduced in Section 4. The further developed method was used
583 to compare the performance of envelops with and without PCM. Future studies may
584 include validating the proposed method for other types of PCM or other materials with
585 varying thermal properties, e.g. loose coal and asphalt cement, with a consideration of
586 using it in the optimization process of PCM in buildings.

587

588 **Acknowledgements**

589

590 This work is supported by the National Natural Science Foundation of China (Grant
591 Nos. 51368060 and 51578012) and Doctoral Innovation Foundation of Beijing
592 University of Technology.

593

594 **References**

595

596 [1] Pomianowski M, Heiselberg P, Zhang YP. Review of thermal energy storage
597 technologies based on PCM application in buildings. Energ Buildings. 2013;67:56-69.
598 [2] Oro E, De Gracia A, Castell A, Farid MM, Cabeza LF. Review on phase change
599 materials (PCMs) for cold thermal energy storage applications. Appl Energ.
600 2012;99:513.
601 [3] Zhou D, Zhao CY, Tian Y. Review on thermal energy storage with phase change
602 materials (PCMs) in building applications. Appl Energ. 2012;92:593-605.
603 [4] Kuznik F, David D, Johannes K, Roux JJ. A review on phase change materials

integrated in building walls. Renew Sust Energ Rev. 2011;15:379-91.
[5] Singh SP, Bhat V. Applications of organic phase change materials for thermal comfort in buildings. Rev Chem Eng. 2014;30:521-38.
[6] Karim L, Barbeon F, Gegout P, Bontemps A, Royon L. New phase-change material components for thermal management of the light weight envelope of buildings. Energ Buildings. 2014;68:703-6.
[7] Li SH, Zhong KC, Zhou YY, Zhang XS. Comparative study on the dynamic heat transfer characteristics of PCM-filled glass window and hollow glass window. Energ Buildings. 2014;85:483-92.
[8] Barreneche C, Navarro ME, Fernandez AI, Cabeza LF. Improvement of the thermal inertia of building materials incorporating PCM. Evaluation in the macroscale. Appl Energ. 2013;109:428-32.
[9] Alvarez S, Cabeza LF, Ruiz-Pardo A, Castell A, Tenorio JA. Building integration of PCM for natural cooling of buildings. Appl Energ. 2013;109:514-22.
[10] Chen C, Guo HF, Liu YN, Yue HL, Wang CD. A new kind of phase change material (PCM) for energy-storing wallboard. Energ Buildings. 2008;40:882-90.
[11] Stazi F, Tomassoni E, Bonfigli C, Di Perna C. Energy, comfort and environmental assessment of different building envelope techniques in a Mediterranean climate with a hot dry summer. Appl Energ. 2014;134:176-96.
[12] Borderon J, Virgone J, Cantin R. Modeling and simulation of a phase change material system for improving summer comfort in domestic residence. Appl Energ. 2015;140:288-96.
[13] Ascione F, Bianco N, De Masi RF, de' Rossi F, Vanoli GP. Energy refurbishment of existing buildings through the use of phase change materials: Energy savings and indoor comfort in the cooling season. Appl Energ. 2014;113:990-1007.
[14] Cheng WL, Xie B, Zhang RM, Xu ZM, Xia YT. Effect of thermal conductivities of shape stabilized PCM on under-floor heating system. Appl Energ. 2015;144:10-8.
[15] Ling HS, Chen C, Wei S, Guan Y, Ma CW, Xie GY, et al. Effect of phase change materials on indoor thermal environment under different weather conditions and over a long time. Appl Energ. 2015;140:329-37.
[16] Shi X, Memon SA, Tang WC, Cui HZ, Xing F. Experimental assessment of position of macro encapsulated phase change material in concrete walls on indoor temperatures and humidity levels. Energ Buildings. 2014;71:80-7.
[17] Castell A, Farid MM. Experimental validation of a methodology to assess PCM effectiveness in cooling building envelopes passively. Energ Buildings. 2014;81:59-71.
[18] Evola G, Marletta L, Sicurella F. A methodology for investigating the effectiveness of PCM wallboards for summer thermal comfort in buildings. Build Environ. 2013;59:517-27.
[19] Zhou T, Darkwa J, Kokogiannakis G. Thermal evaluation of laminated composite phase change material gypsum board under dynamic conditions. Renew Energ. 2015;78:488-56.
[20] Mandilaras I, Stamatiadou M, Katsourinis D, Zannis G, Founti M. Experimental thermal characterization of a Mediterranean residential building with PCM gypsum board walls. Build Environ. 2013;61:93-103.

[21] Zhou GB, Yang YP, Wang X, Cheng JM. Thermal characteristics of shape-stabilized phase change material wallboard with periodical outside temperature waves. Appl Energ. 2010;87:2666-72.
[22] Zhou GB, Yang YP, Xu H. Performance of shape-stabilized phase change material wallboard with periodical outside heat flux waves. Appl Energ. 2011;88:2113-21.
[23] CABR. Thermal Design Code for Civil Building (GB 50176-201X). Beijing: China Building Industry Press; 2014.
[24] Wang JW, Li SH, Guo SR, Ma CW, Wang J, Jin S. Simulation and optimization of solar greenhouses in Northern Jiangsu Province of China. Energ Buildings. 2014;78:143-52.
[25] Kong FH, Zhang QL. Effect of heat and mass coupled transfer combined with freezing process on building exterior envelope. Energ Buildings. 2013;62:486-95.
[26] Feng Y. Thermal design standards for energy efficiency of residential buildings in hot summer/cold winter zones. Energ Buildings. 2004;36:1309-12.
[27] Yan QS, Zhao QZ. Building thermal processes. Beijing: China Building Industry Press; 1986.
[28] Chen C, Liang L, Zhang Y, Chen ZG, Xie GY. Heat transfer performance and structural optimization design method of vertical phase change thermal energy storage device. Energ Buildings. 2014;68:679-85.
[29] Lee KO, Medina MA, Raith E, Sun XQ. Assessing the integration of a thin phase change material (PCM) layer in a residential building wall for heat transfer reduction and management. Appl Energ. 2015;137:699-706.
[30] NREL. EnergyPlus. https://energyplus.net/.2015.
[31] Cheng R, Pomianowski M, Wang X, Heiselberg P, Zhang YP. A new method to determine thermophysical properties of PCM-concrete brick. Appl Energ. 2013;112:988-98.
[32] Goldberg D. Fundamentals of Chemistry (5th Edition ed.): McGraw-Hill; 2006.
[33] Rayleigh L. On the question of the stability of the flow of liquids. Philos Mag. 1892;34:59-70.
[34] Ling HS, Chen C, Guan Y, Wei S, Chen ZG, Li N. Active heat storage characteristics of active-passive triple wall with phase change material. Sol Energy. 2014;110:276-85.
[35] Guan Y, Chen C, Han YQ, Ling HS, Yan QY. Experimental and modelling analysis of a three-layer wall with phase-change thermal storage in a Chinese solar greenhouse. J Build Phys. 2015;38:548-59.
[36] Holman JP. Heat Transfer (9th edition). New York: McGraw Hill; 2002.

Tables with Captions

Table 1: Physical parameters of materials

Material	Thickness m	Density kg/m^3	Thermal conductivity W/(m °C)	Specific heat J/(kg °C)	Solar transmittance %	Visible transmittance %
Block brick	0.8	1800	0.81	1050	-	-
Polystyrene board	0.05	30	0.04	1380	-	-
EVAC film	0.001	-	0.76	-	85	84
Cotton blanket	0.04	-	0.07	-	-	-

Table 2: Simulation conditions

Case	Thickness mm	Density kg/m^3	Thermal conductivity W/(m °C)	Effective equivalent specific heat kJ/(kg °C)
1	50	900	0.56	7.16
2	200	900	0.54	7.16
3	200	100, 200, 300, 400, 600, 1000, 1800, 2500	0.54	7.06±0.95
4	200	900	0.1, 0.2, 0.3, 0.54, 0.7, 1.0, 1.5, 2.0	7.21±0.93
5	200	900	0.54	0.97, 1.60, 3.70, 7.16, 9.10, 11.28, 13.51, 15.70

Table 3: Calculated thermal properties of materials

Material	Thermal conductivity W/(m °C)	Density kg/m^3	(Effective equivalent) special heat kJ/(kg °C)	Thermal storage coefficient W/(m^2°C)
PCM	0.54	900	7.42	16.20
Soil	1.16	2000	1.01	13.05
Block bricks	0.81	1800	1.05	10.54
Polystyrene boards	0.04	30	1.38	0.36

Table 4: Calculated thermal resistance and thermal inertia index of different building envelops

Type	Construction	Thermal resistance		Thermal inertia index	
		Value $m^2°C/W$	Growth rate %	Value	Growth rate %
1	800mm thick block bricks +50mm thick polystyrene boards	2.24	22.07	10.86	47.93
	800mm thick PCM +50mm thick polystyrene boards	2.73		16.06	
2	610mm thick block bricks +50mm thick polystyrene boards	2.00	18.80	8.39	47.32
	610mm thick PCM +50mm thick polystyrene boards	2.38		12.36	
3	370mm thick block bricks +50mm thick polystyrene boards	1.71	13.38	5.26	45.73
	370mm thick PCM +50mm thick polystyrene boards	1.94		7.67	
4	120mm thick block bricks +50mm thick polystyrene boards	1.40	5.30	2.01	38.81
	120mm thick PCM +50mm thick polystyrene boards	1.47		2.79	

Figure Captions

Fig.1. Correlation between the equivalent specific heat of PCM and their temperature.

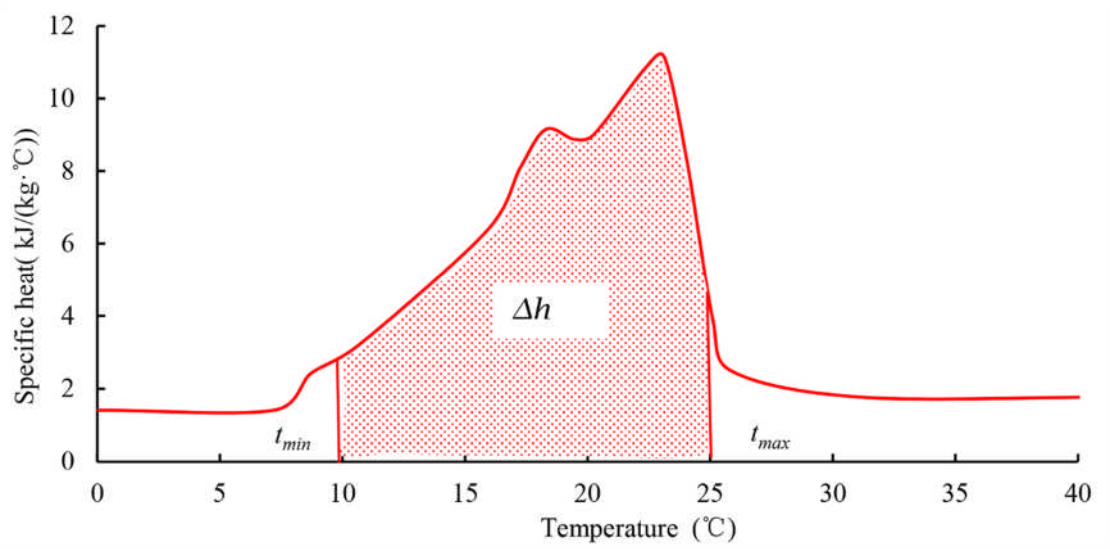

Fig. 2. Schematic diagrams of the investigated solar greenhouse: (a) model of the simulated building, (b) profile map.

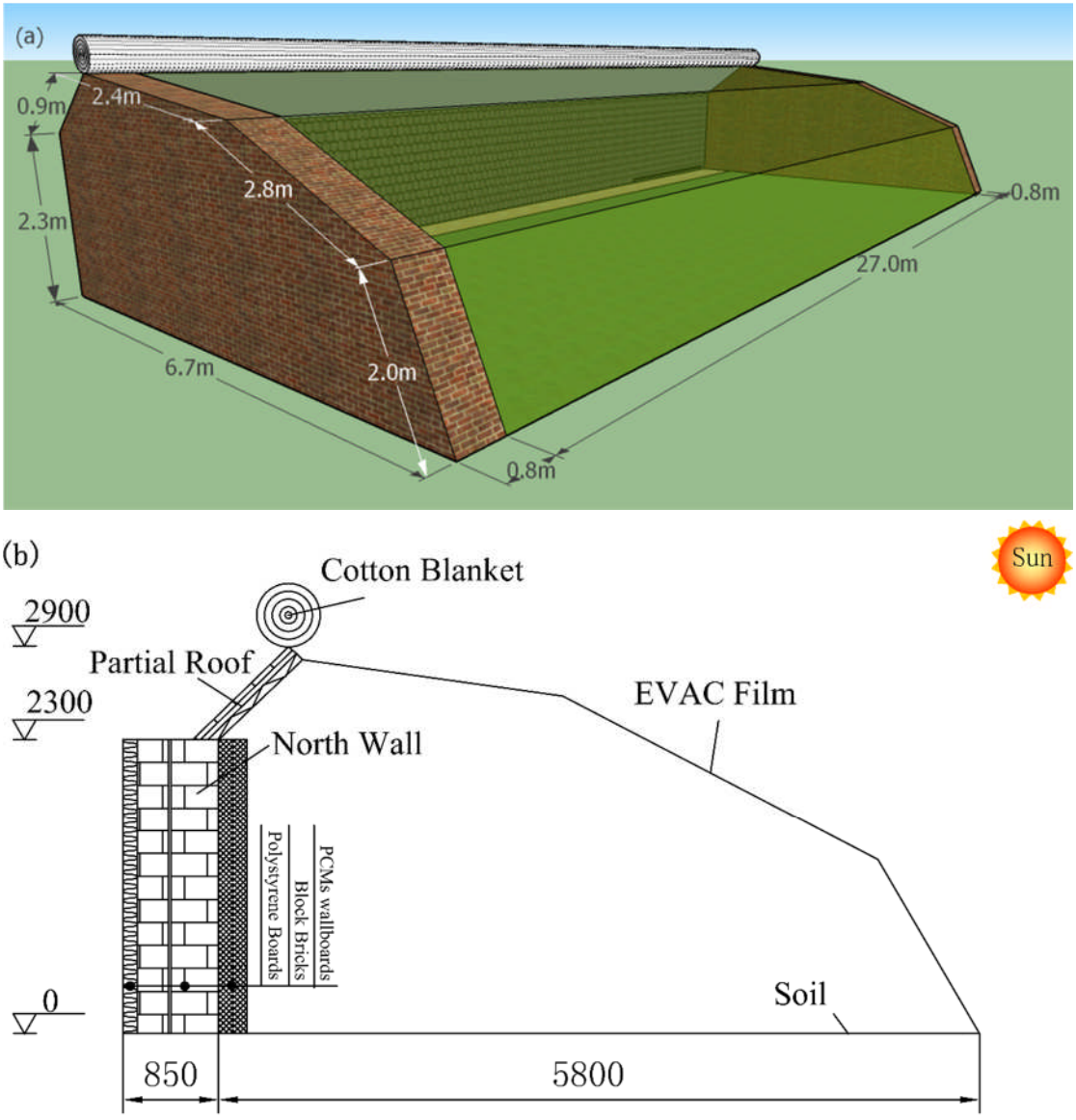

Fig. 3. Hourly outdoor air temperature and solar radiation.

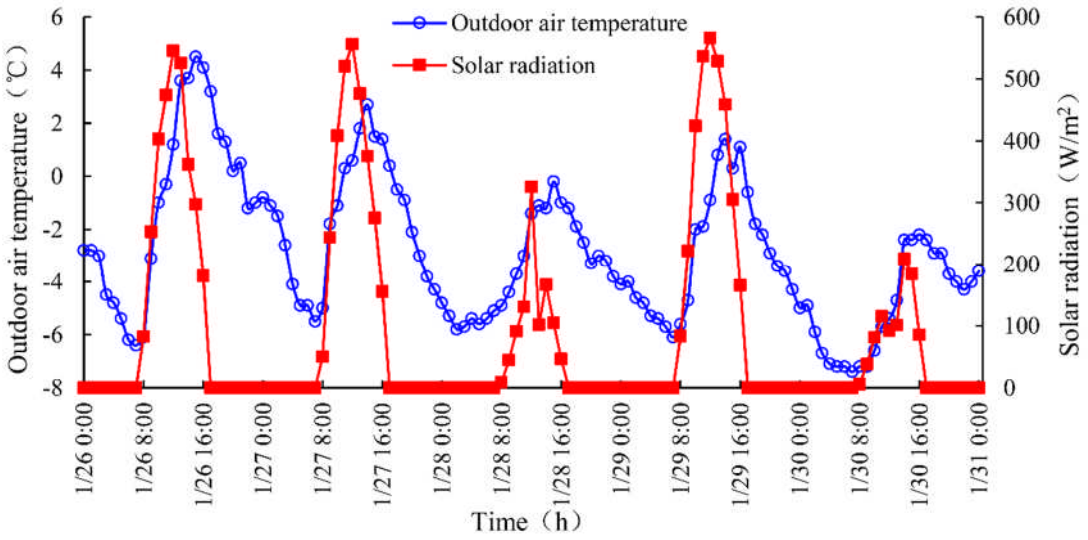

Fig. 4. Measured and calculated surface temperature of PCM.

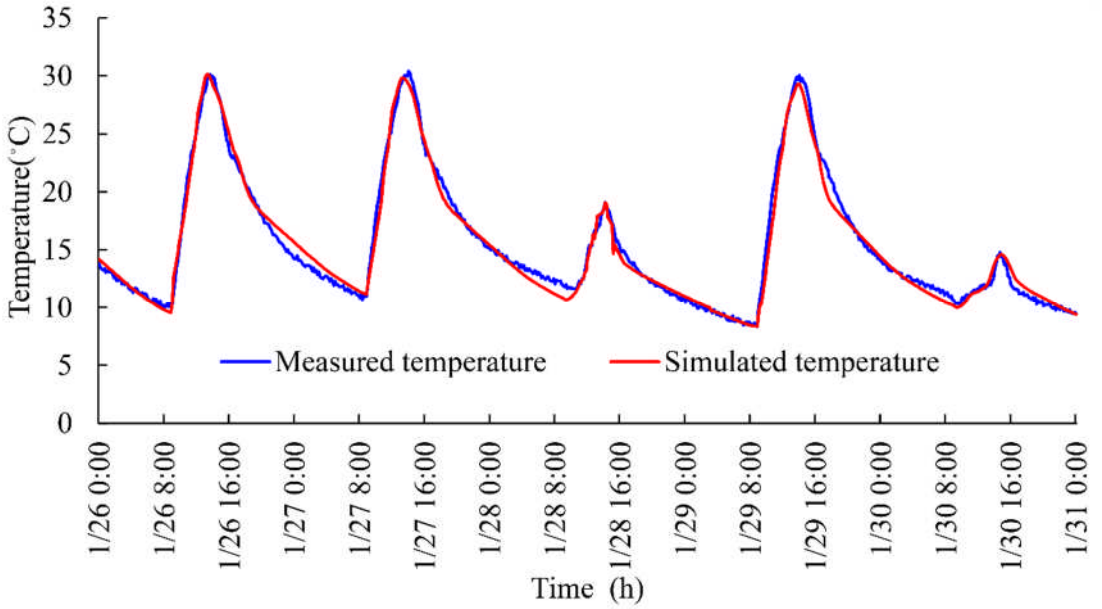

Fig. 5. Temperature distribution along the thickness direction with increase of material thickness.

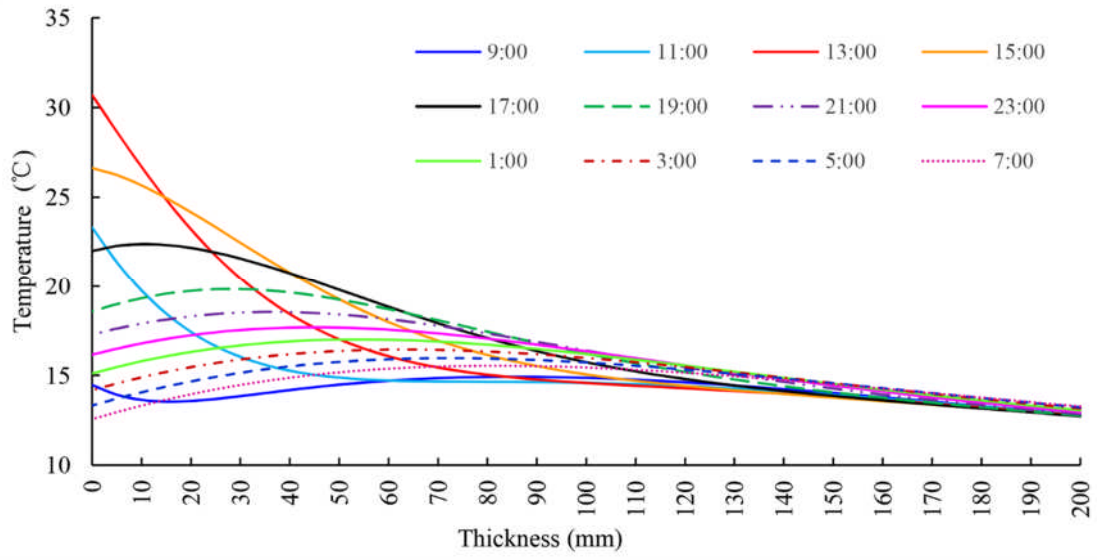

Fig. 6. Thermal storage coefficient, surface heat flux and temperature amplitudes for different density.

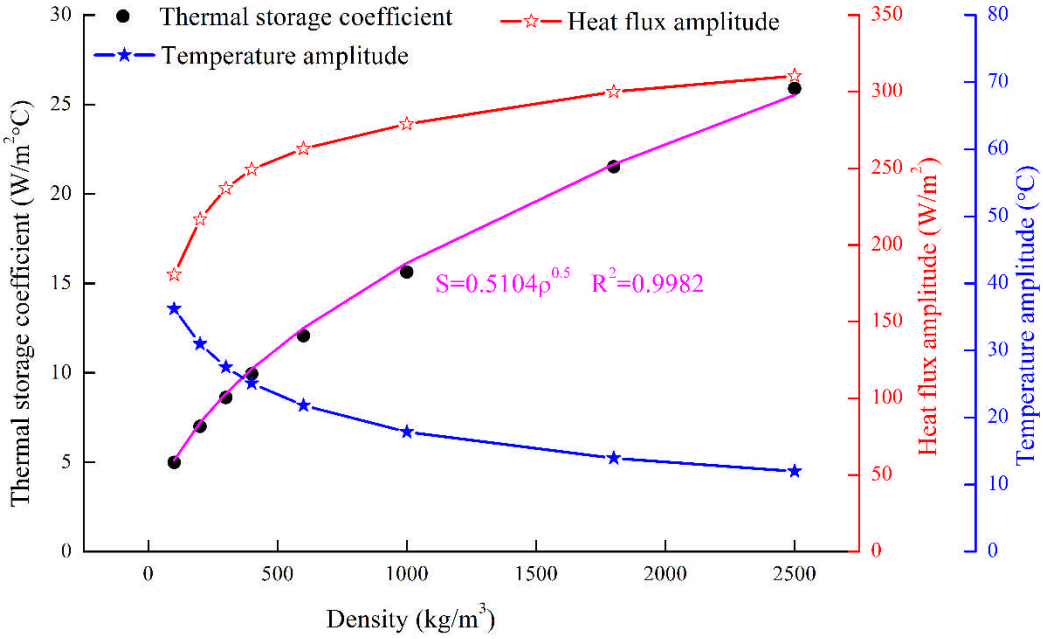

Fig. 7. Thermal storage coefficient, surface heat flux and temperature amplitudes for different thermal conductivity.

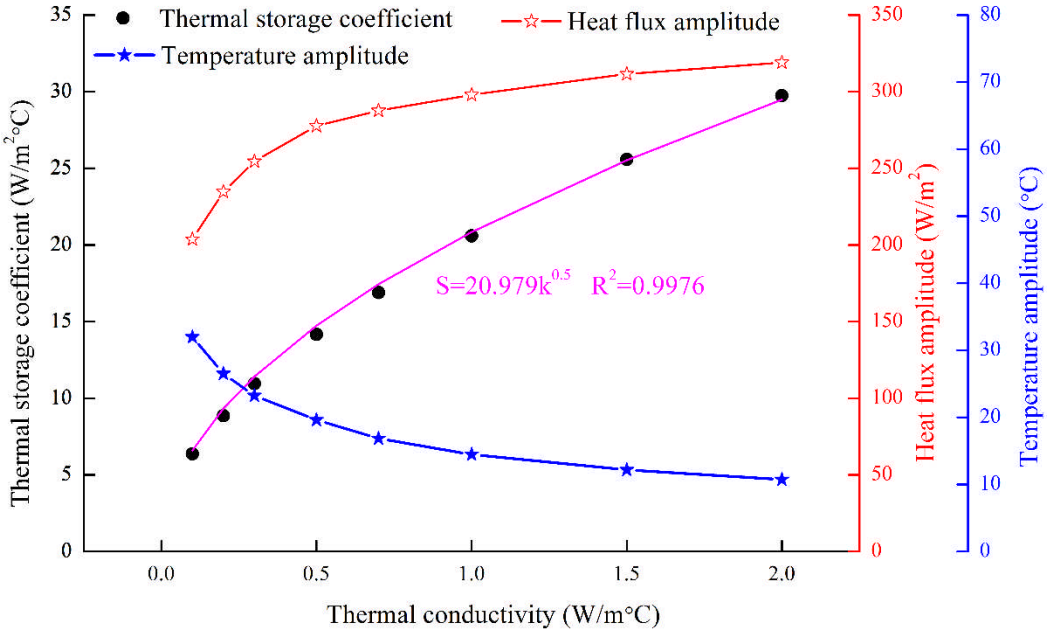

Fig. 8. Thermal storage coefficient, surface heat flux and temperature amplitudes for different effective equivalent specific heat.